Developmental Cell, Vol. 4, 191–204, February, 2003, Copyright ©2003 by Cell Press

Cholesterol Modification of Hedgehog Is Required for Trafficking and Movement, Revealing an Asymmetric Cellular Response to Hedgehog

Armel Gallet,[1] Ralph Rodriguez,[1] Laurent Ruel, and Pascal P. Therond*
Institute of Signaling, Developmental Biology and Cancer Research
CNRS UMR 6543
Centre de Biochimie
Parc Valrose
06108 Nice Cedex 02
France

Summary

Hedgehog family members are secreted proteins involved in numerous patterning mechanisms. Different posttranslational modifications have been shown to modulate Hedgehog biological activity. We investigated the role of these modifications in regulating subcellular localization of Hedgehog in the *Drosophila* embryonic epithelium. We demonstrate that cholesterol modification of Hedgehog is responsible for its assembly in large punctate structures and apical sorting through the activity of the sterol-sensing domain-containing Dispatched protein. We further show that movement of these specialized structures through the cellular field is contingent upon the activity of proteoglycans synthesized by the heparan sulfate polymerase Tout-Velu. Finally, we show that the Hedgehog large punctate structures are necessary only for a subset of Hedgehog target genes across the parasegmental boundary, suggesting that presentation of Hedgehog from different membrane compartments is responsible for Hedgehog functional diversity in epithelial cells.

Introduction

Hedgehog (Hh) family proteins are secreted molecules that function as organizers in animal development (Ingham and McMahon, 2001). Hh proteins signal over several cell diameters in a direct and concentration-dependent manner. However, their movement is subject to tight regulation through posttranslational modifications. In recent years, the role of these modifications in Hh propagation within a cellular field has come under intense scrutiny.

All Hh family proteins follow the same maturation process in Hh-producing cells. Autoproteolytic cleavage occurs under the control of the C-terminal domain of the protein. Concomitantly, a cholesterol moiety is added to the C terminus of the N-terminal domain to give rise to the active Hh, termed Hh-Np ("p" stands for processed). This cholesterol modification allows Hh-Np to be tightly linked to the cell surface. Strikingly, Hh-Np appears to display all the morphogenetic functions for local and long-range signaling, while the C-terminal domain, which is secreted, does not (Beachy et al., 1997, and the references therein).

Numerous questions have been raised about the role of the cholesterol adduct on Hh function. How could the cholesterol modification fit in with both the short- and long-range Hh activities? Several reports have shown that, when Hh is expressed from a transgene that encodes only the N-terminal domain, it does not undergo cleavage and is not linked to cholesterol. In *Drosophila*, this unmodified form, Hh-N, can diffuse further away than Hh-Np (Porter et al., 1996; Burke et al., 1999). Moreover, it has been shown that the *tout-velu* (*ttv*) gene, identified in *Drosophila*, is required for Hh-Np diffusion (Bellaiche et al., 1998; Thé et al., 1999). This gene encodes a GAG transferase enzyme homologous to the vertebrate EXT1 gene (Lind et al., 1998). EXT1 is required for the synthesis of specific proteoglycans that compose the extracellular matrix (McCormick et al., 1998). Cholesterol-unmodified Hh-N, but not Hh-Np, is independent of Ttv function for its movement, suggesting that proteoglycans are specifically required for the movement of cholesterol-modified Hh-Np (Thé et al., 1999).

Recently, another gene was implicated in the release of Hh-Np from the producing cells in *Drosophila*. This gene, *dispatched* (*disp*), belongs to a new family of sterol-sensing domain (SSD)-containing proteins present in vertebrates and invertebrates (Kuwabara and Labouesse, 2002; Ma et al., 2002). Disp was shown to be required for secretion of Hh-Np in *Drosophila* imaginal discs (Burke et al., 1999). In the absence of Disp function, Hh-Np accumulates in producing cells and fails to stimulate its target genes in anterior receiving cells. Conversely, cholesterol-unmodified Hh-N can be secreted in the absence of Disp function, eliciting its effects throughout the wing disc. These results suggest a model in which cholesterol is required for restricting Hh-Np diffusion and controlling its range of action through *disp* and *ttv* activities. In contrast to the *Drosophila* results, an elegant study in developing mouse limb buds (Lewis et al., 2001) has shown that the cholesterol binding to Sonic hedgehog (Shh-Np) is necessary for its long-range function, whereas cholesterol-unmodified Shh-N provides only short-range activity. In agreement with this, in vitro studies from vertebrate cells have shown that Shh-Np can oligomerize, whereas Shh-N cannot. It has been proposed that this multimerization, mediated by the cholesterol moiety, could be required for long-range action of Shh-Np, while absence of cholesterol modification on Shh impairs its oligomerization and, thus, its movement (Zeng et al., 2001).

Another lipid modification on Hh, a palmitoylation of its N-terminal cysteine, has been shown to occur in vertebrates (Cys24) and in *Drosophila* (Cys85) (Pepinsky et al., 1998; Chamoun et al., 2001). The palmitic acid modification of Shh can potentiate its activity in vitro, while palmitic acid modification is dispensable for certain Shh functions in vivo (Pepinsky et al., 1998; Kohtz et al., 2001; Lee et al., 2001; Taylor et al., 2001). Recently several groups have identified the gene responsible for

*Correspondence: therond@unice.fr
[1]These authors contributed equally to this work.

Hh palmitoylation in *Drosophila*. This gene (Jeong and McMahon, 2002, and the references therein) encodes a transmembrane protein sharing similarities with the mammalian acyltransferase that catalyzes O-linked acyl transfers. Abolishing its function in *Drosophila* wing discs mimics an Hh loss-of-function, suggesting that palmitoylation is essential for all Hh functions during wing patterning.

Many studies have focused on the role of the lipid modifications in controlling Hh activity and diffusion during development. Less is known about the possible function of lipid modifications in modulating the sorting and secretion of Hh by producing cells. We report functional experiments providing strong evidence for the role of cholesterol modification on the control of Hh subcellular localization in producing and receiving cells. We used the differentiation of the *Drosophila* embryonic ectoderm as a genetic model to show that cholesterol is required for a Disp-dependent assembly of Hh in large punctate structures. Moreover, Ttv function is necessary for the movement of these structures from the apical surface of producing cells to receiving cells. Finally, we demonstrate that these Hh-enriched structures are required for the activation of target genes across the parasegmental boundary and not for target genes posterior to the Hh source. Thus, we provide in vivo evidence for two different mechanisms of activation of Hh target genes that are dependent on Hh apicobasal sorting that correlates with asymmetric cellular responses to Hh signaling within the ectodermal field.

Results

Asymmetric Target Gene Expression Reflects Direct Hh Activity in the Ventral Ectoderm

We have used the repeated pattern of the *Drosophila* larval ectoderm (which secretes cuticle) to follow Hh activity. Each abdominal segment is composed of two types of cuticle: the naked (or smooth) cuticle and the denticle belts, subdivided into six rows of denticles, easily identifiable by their orientation and shape (Figures 1A and 1P). This cuticle pattern is under the control of several signaling pathways that are indirectly regulated by Hh (Hatini and DiNardo, 2001, and the references therein). Engrailed (En) controls *hh* expression in the two rows of cells that define the posterior compartment of the segment. Across the parasegmental boundary (in cells anterior to the En/Hh domain), Hh maintains *wingless* (*wg*) transcription in one row of cells. The Wg signal then controls the specification of the naked cuticle (Figures 1A, 1B, and 1P). Posterior to the En/Hh domain, Hh initiates *rhomboid* (*rho*) transcription in one to two rows of cells (Figure 1C). *rho* activation induces EGF signaling, allowing differentiation of denticles 1–4 (Figures 1A and 1P). Finally, Hh and Wg are required for *serrate* (*ser*) repression and restrict its expression in three rows of cells posterior to the *rho*-expressing cells. Ser initiates a third row of *rho* expression in adjacent cells (Figures 1D and 1P). The Hh receptor Patched (Ptc) is also transcriptionally upregulated by the Hh pathway in cells on both sides of the En/Hh domain (Figure 1E; Forbes et al., 1993).

Loss of *hh* results in loss of both naked cuticle and denticle diversity (Figure 1F). This cuticle phenotype correlates with Hh target gene expression: loss of *wg* (Figure 1G), extension of the *ser* expression domain, which now covers most of the segment (Figure 1I), and absence of *ptc* upregulation (Figure 1J). *rho* expression is strongly reduced, though some remains under the control of Ser (Figure 1H). Conversely, ubiquitous expression of full-length *hh* (Hh^{FL}) in the ectoderm with the GAL4-UAS system (Brand and Perrimon, 1993) induced an expansion over four to five cells of both *wg* and *rho* expression in the anterior and posterior directions, respectively (Figures 1L and 1M), while *ser* expression was completely repressed (Figure 1N). *ptc* was upregulated in most cells (Figure 1O). Accordingly, the denticle belts of these embryos contained several rows of type 2 denticles, reflecting a uniform level of *rho* expression in response to a uniform level of Hh (Figure 1K).

Thus, *wg*, *rho*, *ser*, and *ptc* expressions reflect direct Hh activity in cells anterior and posterior to *en/hh*-expressing cells (see also Hatini and DiNardo, 2001; Forbes et al., 1993).

Cholesterol Modification of Hh Is Required for Correct Signaling in Anterior Cells, but Not in Posterior Cells

Two endogenous Hh isoforms are present in vivo: one bearing both posttranslational lipid modifications and another modified only by a cholesterol adduct (Chamoun et al., 2001). To address the role of these different modifications in Hh signaling, we assessed the biological activity of different Hh constructs that do not undergo all modifications.

All Hh constructs used in this study have a similar level of expression (data not shown). Our reference transgenic strain expressed Hh^{FL}, which, after cleavage, yields cholesterol-modified Hh-Np that could also be palmitoyled (Figure 2). This construct, like others described below, was ubiquitously expressed with the *69BGal4* driver and tested for its ability to rescue loss of *hh* function. Hh-Np restored *hh*-induced loss of naked cuticle and denticle diversity (compare Figure 2A with Figure 1F). Target gene expression reflected this rescue: three to four rows of *wg*-expressing cells anterior to the En/Hh domain were observed (Figure 2E). Posteriorly, four to five cell rows of *rho*-expressing cells were induced, and *ser* expression was totally repressed (Figures 2I and 2M).

A similar phenotype was observed for the C85S-Hh-Np construct that permits cholesterol modification, but not palmitoylation, of Hh (Figure 2B). Nevertheless, target gene expression was less-potently rescued by this construct (Figures 2F, 2J, and 2N). *wg* expansion was developmentally delayed (data not shown). Activation of *rho* and repression of *ser* were less efficient. We conclude that absence of palmitoylation decreases the overall potency of Hh, as previously shown in vertebrate systems (Pepinsky et al., 1998; Kohtz et al., 2001; Lee et al., 2001; Taylor et al., 2001).

Cholesterol-unmodified Hh-N rescued denticle diversity, but embryos still presented abdominal denticle belt fusions (between two and three per embryo; Figure 2C). Consistently, Hh-N was unable to fully rescue *wg* expression in all segments but could widen the domains

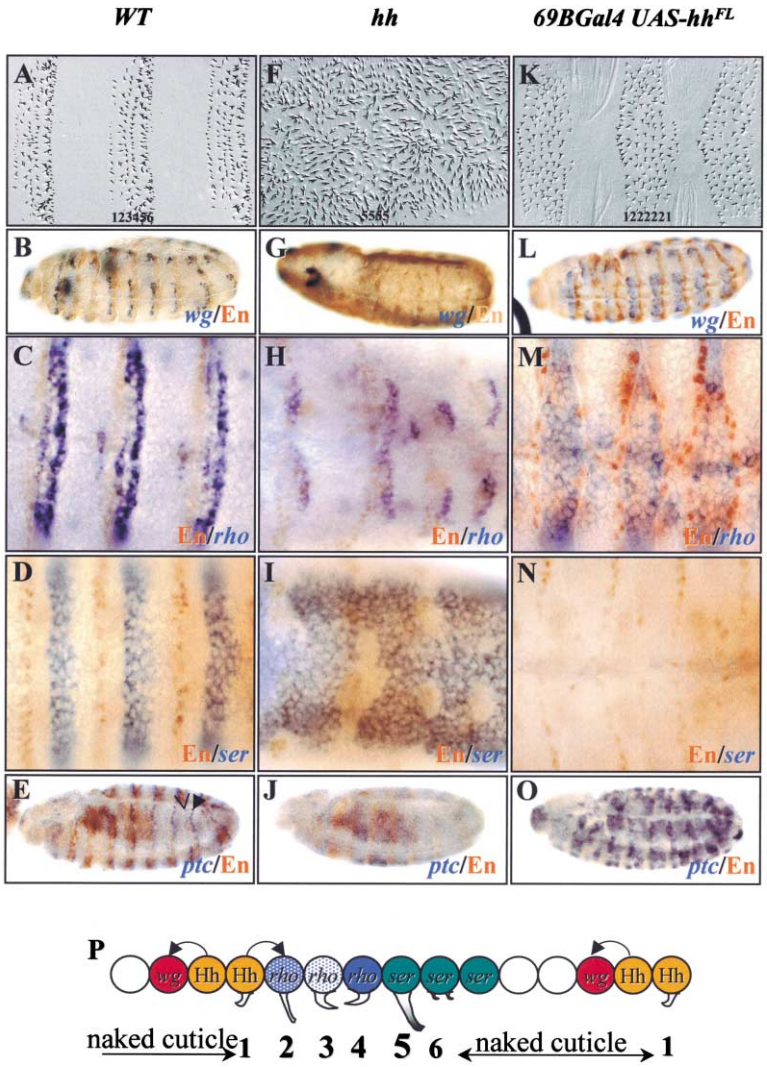

Figure 1. Targets of Hh Activity in the Ventral Ectoderm

Anterior is to the left in all figures.
(A–E) Wild-type embryos.
(F–J) hh^{AC}/hh^{AC} embryos.
(K–O) *69Bgal4 UAS-*hh^{FL} embryos.
(A, F, and K) Cuticle views of first instar larvae with numbers indicating denticle identity.
Blue, mRNA in situ hybridization for *wg* (B, G, and L), *rho* (C, H, and M), *ser* (D, I, and N), and *ptc* (E, J, and O); brown, immunostaining for En protein. (B), (E), (G), (J), (L), and (O) are stage 11 embryos. (C), (D), (H), (I), (M), and (N) are stage 13 embryos.
(P) Scheme representing the expression of Hh target genes and the corresponding cell fate in wild-type larvae.
In an *hh* loss-of-function mutant, *wg* expression is no longer maintained (G), *rho* activation is dramatically reduced (H), *ser* expression is now present in most cells (I), and *ptc* is no longer upregulated on both sides of the Hh source (J). Note that a basal level of *ptc* is still present. Consistently naked cuticle and denticle diversity are absent; only type 5 denticle is observable (F). Ubiquitous expression of wild-type Hh (Hh^{FL}) with the *69Bgal4* driver leads to an expansion of *wg* (L), *rho* (M), and *ptc* (O) expression and to *ser* repression (N). In consequence, only denticles type 1 and 2 are formed (K).

of *rho* expression and *ser* repression (Figures 2G, 2K, and 2O). We also analyzed the behavior of another Hh construct in which the cholesterol adduct had been replaced by another membrane-anchored domain. In this construct, the Hh-N coding sequence is fused to the transmembrane domain of the rat CD2 protein (Hh-N-CD2; Strigini and Cohen, 1997). Importantly, Hh-N-CD2 was unable to induce *wg* expression, while it still stimulated *rho* transcription (Figures 2H and 2L). Consequently, *rho*-dependent denticle diversity was restored (compare Figure 2D with Figure 1F), while no naked cuticle was present. In Figure 2L, most *en* cells are absent, but *rho* is evenly expressed, confirming that its expression is directly dependent on Hh activity and not on a secondary signal coming from *en* cells. Moreover, we can also exclude Ser-dependent *rho* expression, since *ser* expression is fully repressed in these embryos (Figure 2P). In another construct, the cholesterol binding site of Hh was replaced with another lipophilic linkage domain, the glycosyl-phosphatidylinositol (GPI) anchoring signal of *Drosophila* Fasciclin 1 (Hh-N-GPI; Burke et al., 1999). Similar phenotypes were observed with this protein (data not shown).

To assess whether the differences between *wg* and *rho* regulation could be accounted for by differential sensitivity to Hh levels, we analyzed *ptc*, which is expressed on both sides of Hh-secreting cells. The different constructs were expressed in the endogenous Hh domain with the *enGal4* driver in an *hh* null background. The initiation of *en* expression is independent of Wg activity and is sufficient to transiently express the Gal4 protein and, thus, the UAS transgene independently of the Hh and Wg regulatory loop (Heemskerk et al., 1991). In these embryos, *ptc* is always upregulated in cells posterior to the Hh source (Figures 2Q–2T, thick arrows). However, anterior upregulation of *ptc* is always weaker (Figures 2Q and 2R, thin arrows), as observed for anterior *ptc* activation by endogenous Hh in wild-type embryos (Figure 1E, thin arrow). Furthermore, anterior *ptc* activation is largely absent in embryos expressing non-cholesterol-modified Hh-N (Figure 2S). This effect is enhanced when Hh-N-CD2 is expressed in *en* cells (Figure 2T). This differential *ptc* upregulation reveals an asymmetric activation process of the Hh pathway on either side of the Hh source.

On the basis of these data, we hypothesized that the

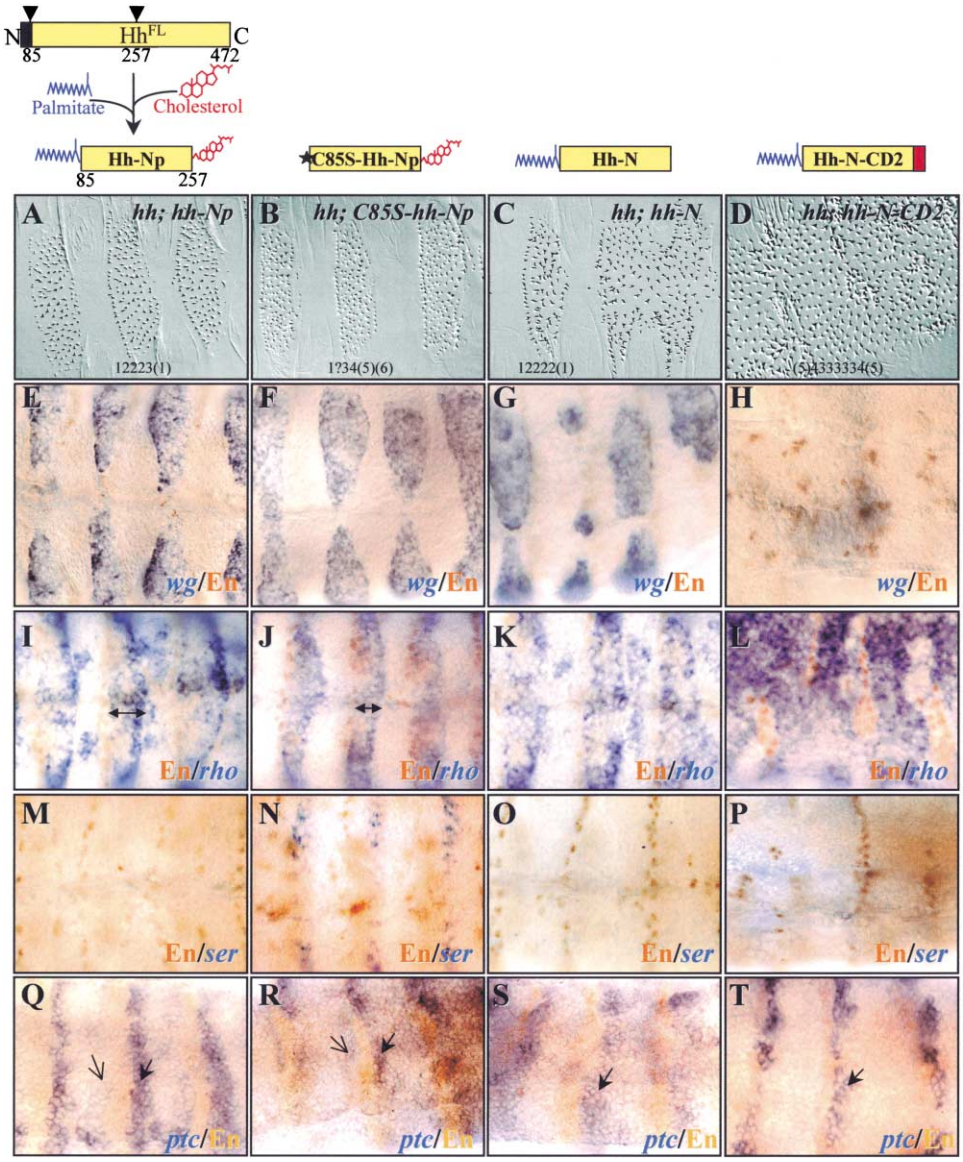

Figure 2. Cholesterol Adduct on Hh Is Necessary for *wg*, but Not for *rho*, Expression

Diagrams of the different Hh constructs are shown on the top. After cleavage (black arrowheads) the *UAS-Hh*^{FL} construct yields the Hh-Np peptide bound to palmitate on the N-terminal Cys85 and to cholesterol on the C-terminal extremity. Analysis of *hh* loss-of-function embryos rescued by the different *UAS-hh* constructs under the ubiquitous *69BGal4* driver (A–P) or under the *enGal4* driver (Q–T): (A, E, I, M, and Q) *hh, UAS-hh-Np*; (B, F, J, N, and R) *hh, UAS-C85S-hh-Np*; (C, G, K, O, and S) *hh, UAS-hh-N*; (D, H, L, P, and T) *hh, UAS-hh-N-CD2*.

(A–D) Cuticle views.

Blue, mRNA in situ hybridization for *wg* (E–H), *rho* (I–L), *ser* (M–P), and *ptc* (Q–T). En-expressing cells are shown in brown.

(E–P) Stage 13 embryos.

(Q–T) Stage 11 embryos.

Hh-Np and C85S-Hh-Np specify naked cuticle differentiation (A and B) by activating broad *wg* transcription (E and F). Hh-N and Hh-N-CD2 are unable to fully rescue naked cuticle (C and D) and *wg* expression (G and H). Conversely, *rho* activation is not affected by the absence of cholesterol (compare [I] and [J] to [K] and [L]) and, in consequence, denticle diversity is rescued (A–D). Note that Hh-N-CD2 is able to induce *rho* expression in almost all cells of the segment (L). Thus, type 5 denticles have almost completely disappeared (D). *ser* is repressed by all Hh constructs (M–P). *ptc* is always upregulated, posterior to the Hh source in a wider and stronger manner (closed arrows) than in anterior cells (open arrows) (Q–T). Note that Hh-N and Hh-N-CD2 are unable to activate *ptc* in cells anterior to the En/Hh domain. Note also that loss of palmitic acid modification reduces Hh potency to activate *rho*, repress *ser*, or upregulate *ptc* (compare [J], [N], and [R] with [I], [M], and [Q]).

differences observed could be accounted for by differential activation mechanisms. Our results outline the important role of the Hh cholesterol modification in stimulating the anterior target genes *wg* and *ptc* across the parasegmental boundary and, subsequently, naked cuticle differentiation, while cholesterol appears dispensable for posterior induction of *ptc* and *rho* and, thus, denticle diversity. Because some *wg* expression can

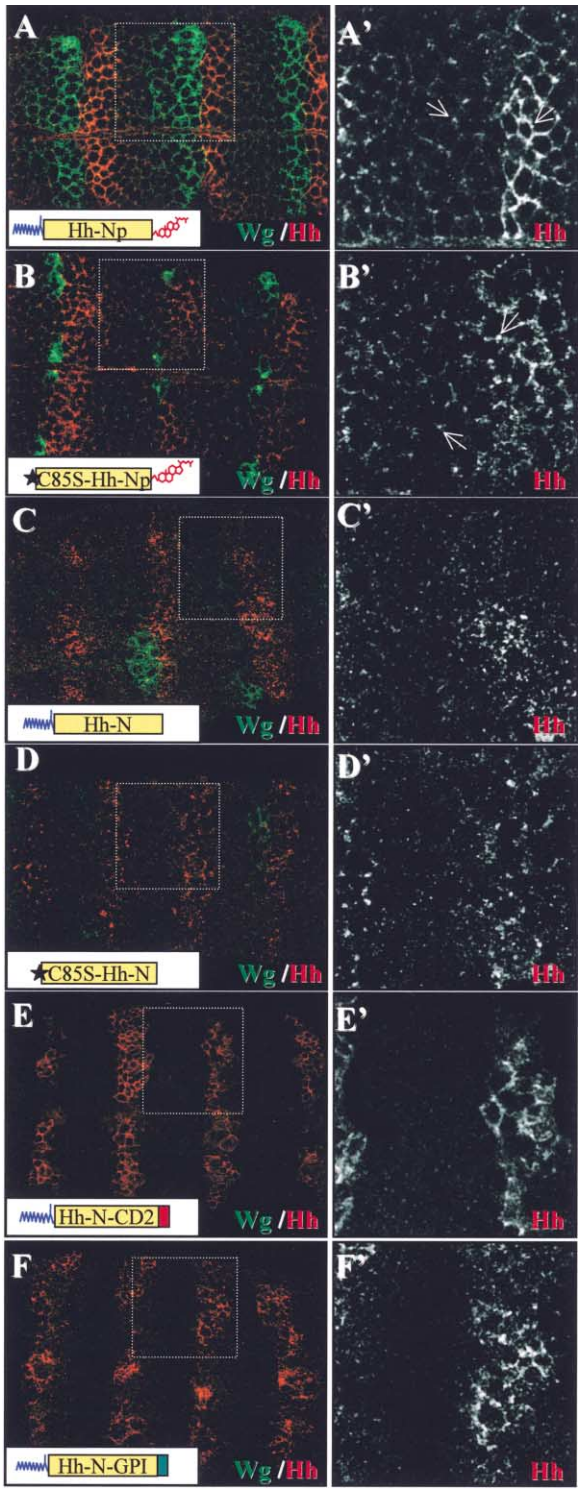

Figure 3. The Cholesterol Moiety Is Necessary for Hh Surface Distribution

(A–F) Stage 11 *hh* mutant embryos expressing different exogenous Hh proteins (diagram in left corners) in En cells and double stained for Wg (green) and Hh (red).

(A′–F′) Enlargements of squares drawn in (A–F) showing only the Hh channel. Hh-Np and C85S-Hh-Np are tightly linked to En-expressing cell membrane (A–B′). Both constructs are also detected in LPSs in and away from producing cells ([A′] and [B′], arrows). Staining of Hh-N and C85S-Hh-N is more diffuse (C–D′). Conversely, Hh-N-CD2 and Hh-N-GPI are always tightly linked to the membrane of producing cells (E–F′). Hh-N-CD2 is uniformly present at the membrane (E and E′), whereas Hh-N-GPI is more concentrated in membrane subdomains (F and F′), but none of these constructs present LPS staining (see also Figure 4). Note that constructs lacking the cholesterol adduct are unable to maintain Wg expression (C–F), whereas constructs modified by cholesterol are able to do so (A and B).

still be activated by Hh-N, the presence of cholesterol modification on Hh might not be the only requirement for anterior target gene regulation. Hh-N-CD2 and Hh-N-GPI activities suggest to us that the differences observed could be a consequence of Hh differential sorting in the producing cells and/or access and presentation to the target cell surface.

The Cholesterol Moiety Is Required for Hh Assembly in Large Punctate Structures

Distribution of Hh within the segmental field was analyzed by confocal microscopy. Each construct was expressed in the endogenous *hh*-expressing domain with the *enGal4* driver. To avoid any endogenous *hh* activity, we tested all constructs in an *hh* null background.

Cholesterol-modified Hh-Np (Figures 3A and 3A′) is mainly present at the producing cell membranes but is also detected far away from its source, as previously described (Tabata and Kornberg, 1994; Taylor et al., 1993; Porter et al., 1996). Interestingly, Hh-Np staining is concentrated in *l*arge *p*unctate *s*tructures (LPSs; Figure 3A′, arrows) in all cells of the segmental field. This staining is also observed for the C85S-Hh-Np construct that permits cholesterol modification, but not acylation, of Hh (Figures 3B and 3B′). This indicates that the absence of acylation on Hh does not impair its subcellular localization (see also below).

The Hh cell membrane localization and LPS staining patterns are strongly impaired when cholesterol-unmodified Hh-N is expressed, instead of Hh-Np (Figures 3C and 3C′). Some smaller dots are present, but they are not associated with membranes and show a more diffuse pattern. Similar staining was observed with an Hh molecule that could not be cholesterol- or palmitoyl-modified (C85S-Hh-N; Figures 3D and 3D′). This suggests that, in vivo, the cholesterol adduct is necessary for Hh localization both at the cell membrane and in LPSs.

To investigate whether Hh localization in LPSs is only a consequence of its membrane association, we examined the surface distribution of Hh-N-GPI and Hh-N-CD2 that are constitutively membrane anchored. Hh-N-CD2 is localized at the cell membrane, but no LPSs were observed in producing or receiving cells (Figures 3E and 3E′). Hh-N-GPI is enriched at the cell membrane in punctate structures that are much smaller than LPSs (Figures 3F and 3F′; see also Figure 4). In addition, Hh-N-GPI cannot be detected far away from the Hh source, except in rare small dots in juxtaposing cells, likely because of endocytosis into neighboring cells. These data argue in favor of a cholesterol-dependent sorting of Hh-Np in a specialized membrane compartment from which

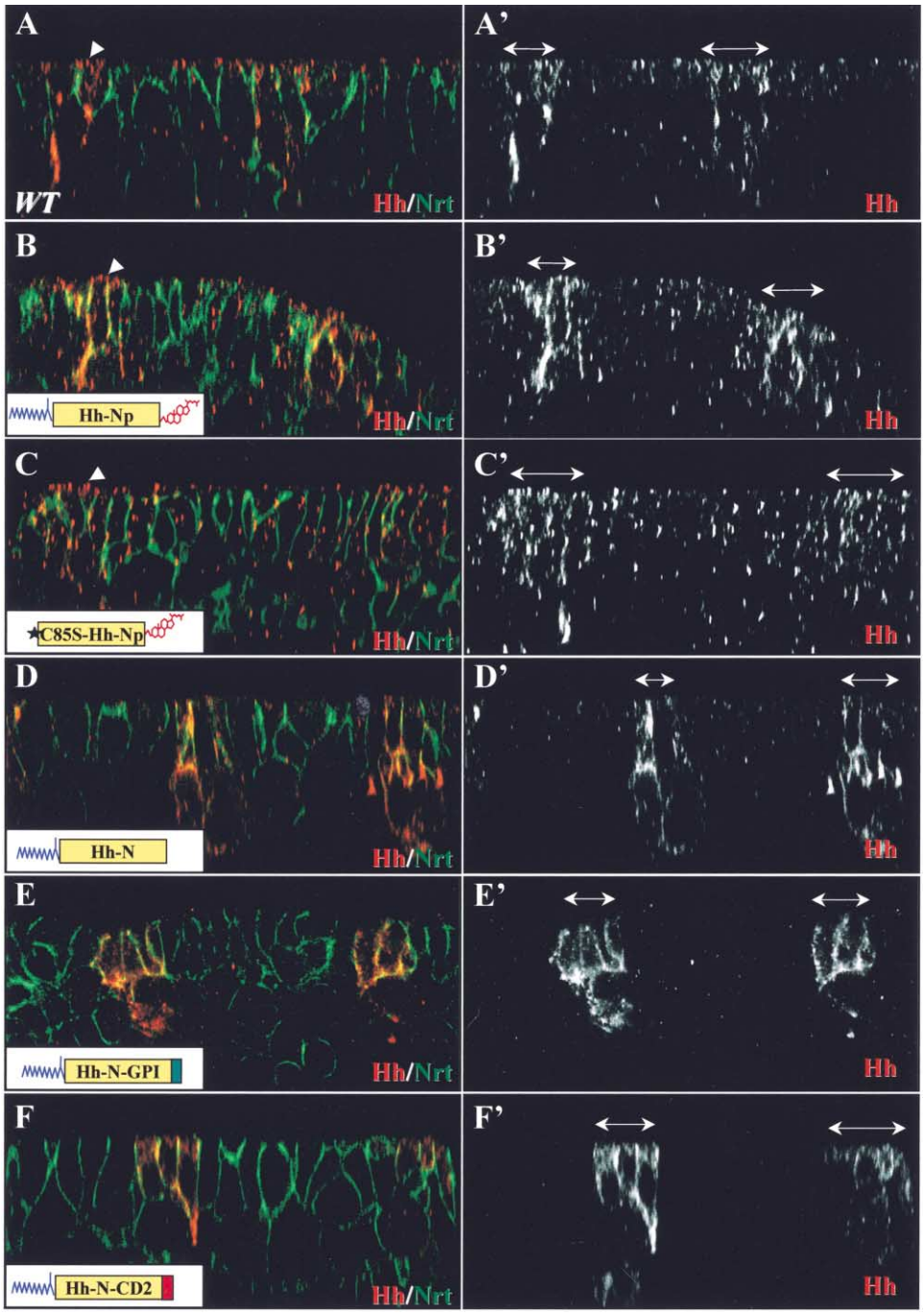

Figure 4. Absence of Cholesterol Modification on Hh Alters Its Distribution in Large Punctate Structures

Subcellular localization of different Hh constructs analyzed by confocal Z sections in ectodermal epithelium of stage 11 embryos. Apical is up, and basolateral is down in all panels.

(A–F) Hh, red; Nrt, green. Nrt marks the basolateral membrane. (A′)–(F′) correspond to the red channel showing Hh staining, with double-headed arrows marking the Hh-producing cells. All constructs are expressed in the *en*-expressing cells. Round cells underneath the ectodermal epithelium are neuronal cells.

(A) WT embryo. Hh is detected both at the apical and basolateral membrane of the producing cells. LPSs are enriched at the apical surface (white arrowheads). LPSs are also present far from their source.

(B and C) Exogenous Hh-Np and C85S-Hh-Np follow the same subcellular localization as endogenous Hh.

(D) In absence of cholesterol modification on Hh (Hh-N), no LPSs are present. Small dots are still observable in both producing and receiving cells.

(E and F) GPI lipid modification and CD2 transmembrane domain target Hh preferentially to the basolateral membrane. Note that no LPSs are detectable when Hh is tethered with GPI or CD2 domains.

the LPSs originate (see below). Note that, as previously shown, constructs that are cholesterol-modified could sustain anterior *wg* expression—although C85S-Hh-Np is less efficient (Figures 3A and 3B)—whereas cholesterol-unmodified constructs failed to maintain it (Figures 3C–3F).

We further analyzed the subcellular localization of Hh constructs by Z sections and double staining with Neurotactin (Nrt), which marks the basolateral membrane of embryonic ectodermal cells (Müller and Wieschaus, 1996).

In wild-type embryos, endogenous Hh-Np is present at the basolateral membrane of producing cells, as previously shown (Figures 4A and 4A′; Taylor et al., 1993; Tabata and Kornberg, 1994; Porter et al., 1996). Strong staining in LPSs is visible at the apical surface (Figure 4A, arrowheads) of producing and receiving cells. LPSs are also detected in the cytosol of expressing and receiving cells and could represent trafficking intermediates. Similar, but stronger, staining is obtained when exogenous Hh-Np and C85S-Hh-Np are expressed in *en* cells (Figures 4B–4C′).

Loss of cholesterol modification dramatically impaired Hh subcellular localization. Although basolateral staining is observed in Hh-N-producing cells, LPSs are barely detectable, particularly the apically located ones (Figure 4D and 4D′). This confirms that cholesterol modification of Hh is required for its assembly into LPSs and strongly suggests that it is required for apical targeting.

We performed similar experiments using either Hh-N-GPI or Hh-N-CD2. Hh-N-GPI is mainly present at the basolateral membrane (Figures 4E and 4E′), as has been observed for other GPI-modified proteins in *Drosophila* epithelia (Greco et al., 2001). Similarly, Hh-N-CD2 is strongly concentrated at the basolateral membrane (Figures 4F and 4F′). Importantly, none of these proteins are located in LPSs. Note that both Hh-N-CD2 and Hh-N-GPI show strong cytosolic staining, likely because of saturation of the trafficking organelles by overexpressed protein.

Taken together, our data demonstrate that cholesterol is required for Hh concentration in LPSs and for its apical targeting in expressing cells. We hypothesized that these structures could be necessary for the access of Hh to anterior cells across the parasegmental boundary present between *en* and *wg* cells.

Dispatched Is Required for Hh-Np Localization in Large Punctate Structures and for Anterior Target Gene Activation

Disp is required for the release of Hh-Np from producing cells in *Drosophila* imaginal discs (Burke et al., 1999), suggesting that it might be involved in Hh-Np assembly into LPSs. In order to test this hypothesis, we analyzed endogenous Hh-Np subcellular localization in embryos lacking both maternal and zygotic *disp* function. In this genetic background, endogenous Hh-Np was not detected in LPSs or at the apical cell surface, but it was present in few small particles, either at the basolateral membrane surface or inside receiving cells (Figures 5D and 5D′).

Expression of exogenous Hh-Np in *en* cells in a *disp* germline clone (glc) mutant background greatly increased Hh-Np accumulation at the basolateral membrane, but, remarkably, LPS staining still could not be observed. However, few small dots of Hh-Np were still visible inside the receiving cells, suggesting that some Hh-Np could reach target cells (Figures 5H and 5H′). In contrast, Hh-N subcellular localization was identical in a *disp* mutant background to that in a wild-type background (compare Figures 5L–5L′ to Figure 4D).

To correlate Hh staining in LPSs with its biological activity, we analyzed *wg* and *rho* expression in the absence of *disp* function. In *disp* mutants, *wg* is lost (Figure 5B; Burke et al., 1999), correlating with the loss of naked cuticle (Figure 5A). Importantly, *rho* expression appears to be less affected than in *hh* loss-of-function embryos (compare Figure 5C with Figure 1H), and, accordingly, denticle diversity is observed (Figure 5A, arrows). When exogenous Hh-Np was expressed in the absence of any *disp* function, the resulting cuticles displayed greatly enhanced denticle diversity (Figure 5E) because of expanded *rho* expression (Figure 5G). However, maintenance of *wg* expression and naked cuticle formation are not rescued (Figures 5E and 5F). Likewise, expansion of the *rho* expression domain and denticle diversity driven by Hh-N is not affected in *disp* mutants (Figures 5I and 5K). Nevertheless, as in previous experiments, Hh-N could not rescue *wg* expression or naked cuticle (Figures 5I and 5J). This confirms that Disp does not restrain Hh-N secretion, as shown in Figure 5L, and that *rho* activation is cholesterol- and *disp*-independent.

These data show that Disp is required for Hh LPS formation and for Hh apical sorting in a cholesterol-dependent manner. The absence of LPSs affects the ability of Hh to activate its anterior target gene, *wg*. However, *disp* function is not required for basolateral Hh targeting or for activation of posterior target genes such as *rho*.

Asymmetric Requirement for Tout-Velu Activity Reveals Its Role in Hh-Np LPS Movement

Hh-Np is tightly linked to the membrane surface because of the cholesterol adduct; therefore, an active diffusion process may be necessary for its movement from the producing cells. Since Ttv is specifically required for the movement of Hh-Np (Bellaiche et al., 1998; Thé et al., 1999), we hypothesized that *ttv* mutations might affect LPS distribution or movement and, consequently, affect *wg*, but not *rho*, expression.

Embryos lacking both maternal and zygotic *ttv* function display weaker cuticlar phenotypes than *hh* embryos with the presence of some denticle diversity (Figure 6A, arrows). In these embryos, *wg* fades (Figure 6B; Thé et al., 1999), but *rho* expression is present in three rows of cells, similar to that in wild-type embryos (compare Figure 6C to Figure 1C). Expression of exogenous Hh-Np in *ttv* mutants enhanced the *rho* expression domain and, consequently, the rescue of denticle diversity, while *wg* expression was still not maintained (Figures 6E–6G). In these embryos, strong apical Hh staining in LPSs as well as a basolateral staining was observed (Figures 6H and 6H′). However, the LPSs were not present outside the source of Hh, as if Hh-Np were retained in producing cells, as observed for endogenous Hh in *ttv* mutants (Figures 6D and 6D′).

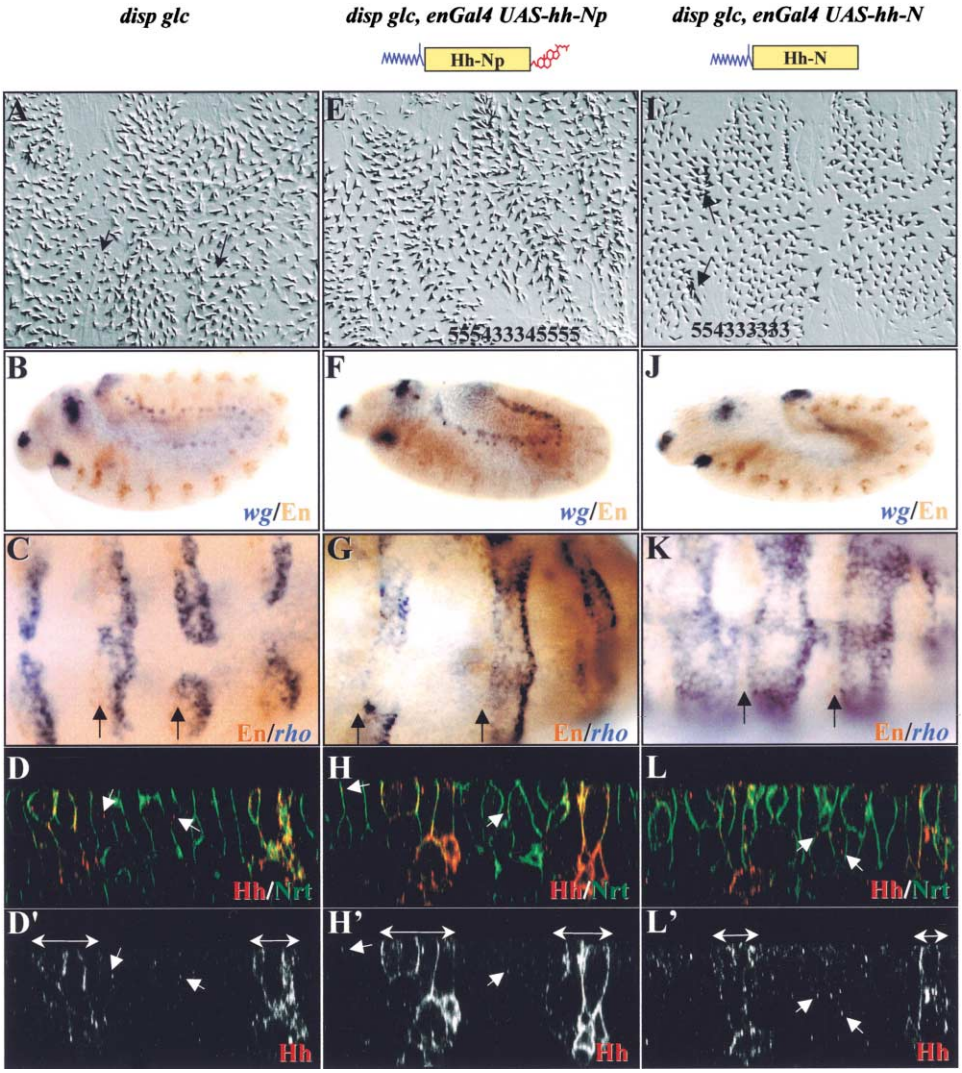

Figure 5. Disp Is Required for *wg* Expression and Hh Assembly in Large Punctate Structures, but Not for *rho* Expression

(A–D′) *disp* glc embryos.

(E–H′) *disp* glc, *enGal4 UAS-hh-Np* embryos.

(I–L′) *disp* glc, *enGal4 UAS-hh-N* embryos.

(A, E, and I) Cuticle views.

(B, D, F, H, J, and L) Stage 11 embryos.

(C, G, and K) Stage 13 embryos. Blue, mRNA in situ hybridization for *wg* (B, F, and J) and *rho* (C, G, and K); brown, En-expressing cells. Arrows indicate the stripes of En-expressing cells that are out of focus.

(D, H, and L) Confocal Z sections of the ectoderm; Hh, red; Nrt, green.

(D′, H′, and L′) Hh staining alone, with white double-headed arrows marking Hh-producing cells.

disp embryos display a weaker phenotype than do *hh* loss-of-function embryos (A). Naked cuticle and *wg* expression are lost (A and B), and small denticles different from type 5 are formed ([A], arrows), reflecting persisting *rho* expression (C). No LPS staining is detected either in producing or receiving cells (D and D′). Note that Hh is present in small particles away from expressing cells (arrows). Expression of Hh-Np in *disp* glc embryos enhances denticle diversity (denticles type 3 and 4; [E]) because of wider *rho* expression (G), but *wg* expression and naked cuticle are still absent (E and F). In these embryos, LPS formation and apical localization of Hh are not rescued (compare [H] and [H′] with Figures 4A and 4B). A strong basolateral staining in producing cells is still observed. Dots of weak Hh staining inside cells away from the Hh source are also detectable ([H] and [H′], arrows). Removing cholesterol modification on Hh (Hh-N) permits a wider expansion of *rho* (K), but no *wg* induction (J). Denticles type 3 and 4 cover each segment, whereas denticles type 5 have almost totally disappeared ([I], arrows), and no naked cuticle is formed. Lack of Disp affects neither the secretion nor the localization of Hh-N (compare [L] and [L′] to Figure 4D).

To confirm the asymmetric cellular response to Hh signaling, we expressed Ttv only in the *wg*-expressing cells of *ttv* mutant embryos (Figure 6I). Strikingly, the ventral cuticle of such embryos is completely rescued, back to wild-type, with formation of denticle types 1–6 and naked cuticle. Furthermore, the Hh gradient is shifted anteriorly in the cellular field (Figures 6J and 6J′) compared with the Hh gradient in wild-type embryos (Figures 6L and 6L′). This confirmed the requirement of Ttv for Hh movement. Analyses of LPS localization clearly showed an asymmetry across En cells. LPSs were present in cells anterior to the En stripe, whereas

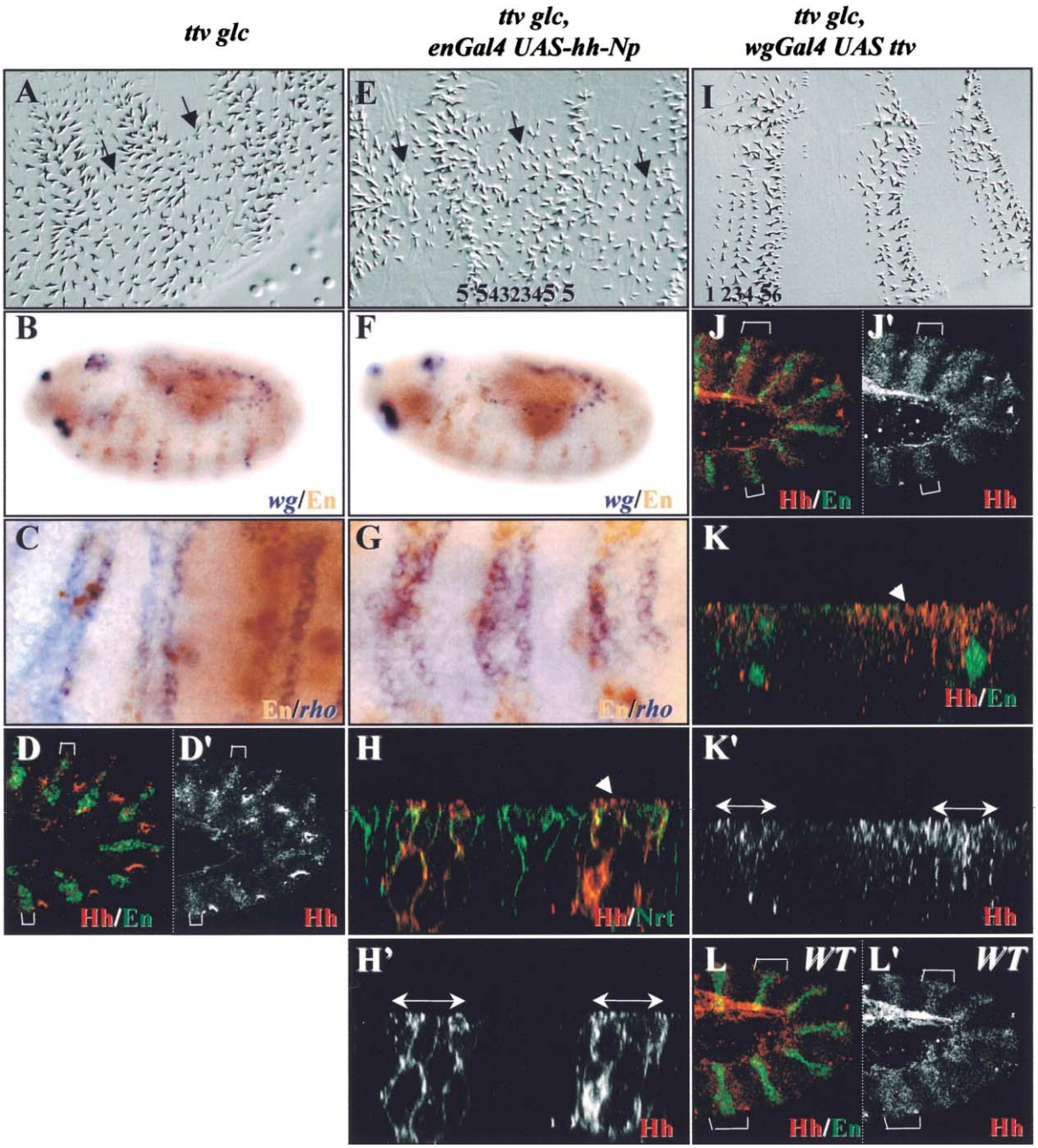

Figure 6. Ttv Is Required for LPS Movement and Anterior Hh Function

(A–D′) *ttv* glc embryos.

(E–H′) *ttv* glc, *enGal4 UAS-hh-Np* embryos.

(I–K′) *ttv* glc, *wgGal4 UAS-ttv* embryos.

(L and L′) Wild-type embryos.

All embryos are at stage 11, except (A), (E), and (I), which are cuticle views, and (C) and (G), which are stage 13 embryos. Blue, mRNA in situ hybridization for *wg* (B and F) and *rho* (C and G); brown, immunostaining for En (B, C, F, and G). In all fluorescent panels, Hh is red, and En (D, J, K, and L) or Nrt (H) is green. (D′), (H′), (L′), (J′), and (K′) show Hh staining alone.

(H and K) Ectodermal confocal Z sections.

ttv loss-of-function embryos do not display any naked cuticle formation (A), even under overexpression of Hh-Np (E), correlating with the absence of *wg* maintenance (B and F). *rho* is still expressed in three rows of cells, as in wild-type embryos (compare Figure 6C to Figure 1C), confirming the observed denticle diversity ([A], arrows). The domain of *rho* expression is wider (four to five rows of cells) when exogenous Hh-Np is expressed (G), resulting in increased denticle diversity ([E], arrows). Confocal Z section of ectodermal cells shows that loss of *ttv* function does not affect Hh-Np basolateral localization or its apical LPS staining ([H], arrowhead) in producing cells ([H′], double arrowheads). However, no Hh is detected outside of producing cells (D, D′, H, and H′). Expression of a *UAS-ttv* transgene in *wg*-expressing cells is sufficient to rescue the *ttv* glc phenotype: naked cuticle and all denticle diversity are restored (I). In consequence, Hh LPSs can now diffuse anteriorly but are still restricted to En cells posteriorly ([J]–[K′], brackets). In wild-type embryos, Hh appears to symmetrically diffuse in both directions from En cells ([L] and [L′], brackets; see also Figures 4A and 4B).

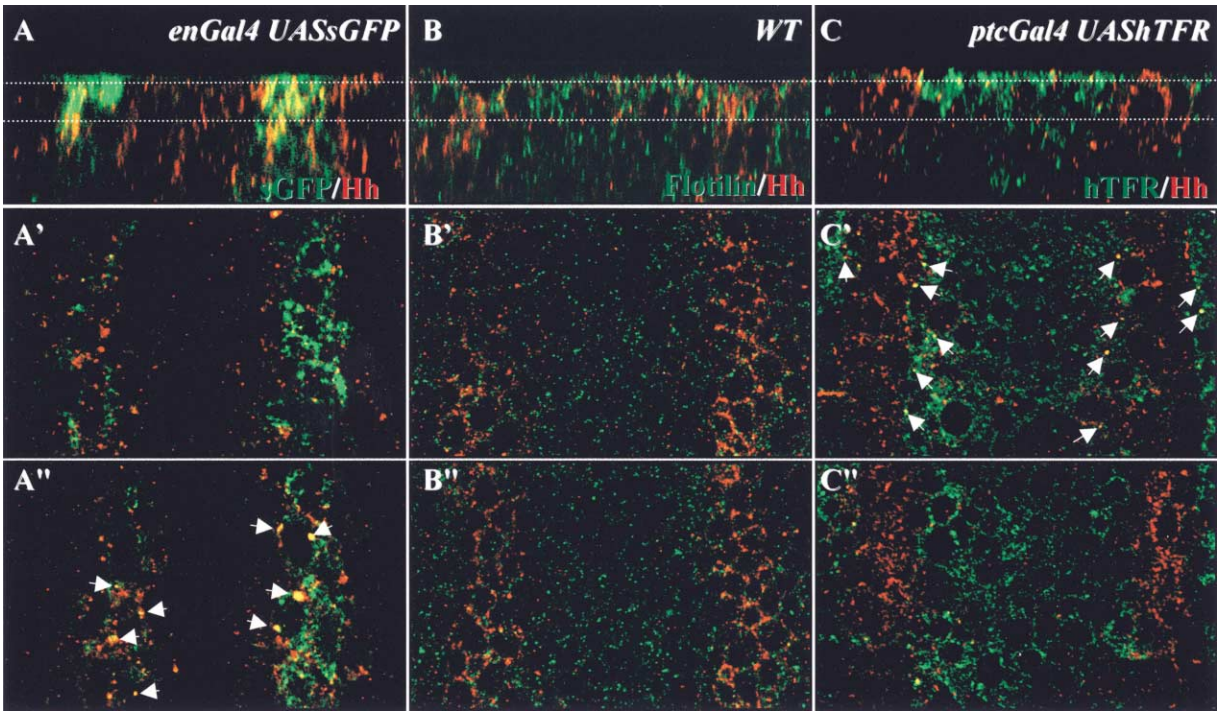

Figure 7. Colocalization of Hh-Np LPS and hTfR during Internalization

(A–A″) *enGal4 UAS-sGFP*, (B–B″) wild-type, and (C–C″) *ptcGal4 UAS-hTfR* stage 10 embryos. (A)–(C) are confocal Z sections of the ectoderm. Upper and lower dashed lines on the Z sections correspond to the apical x/y section and lateral x/y section shown in (A′–C′) and (A″–C″), respectively. Hh is in red in all panels. Green, sGFP (A–A″), Flo^{Dm} (B–B″), and hTfR (C–C″). In producing cells, Hh colocalizes with sGFP in large cytoplasmic secretory vesicles ([A] and arrows in [A″]); however, no apical costaining is visible (A and A′). No colocalization of Hh and Flo^{Dm} is detectable either in producing or in receiving cells (B–B″). Hh colocalizes apically with hTfR in cells adjacent to its source of production, indicating its presence in early endosomes of receiving cells ([C]–[C′], arrows).

they were not observed posterior to the En stripe (Figures 6K and 6K′).

Thus, Ttv is not required for Hh LPS formation and its apical sorting but is necessary for LPS transport or stability between producing and receiving cells. In the absence of Ttv function, the posterior Hh target gene *rho* is still activated independently of LPS movement.

Further Characterization of LPS Movement from Producing to Receiving Cells

We investigated the route used by Hh-Np in secreting cells. A *UAS-sGFP* construct was driven in Hh-expressing cells. sGFP corresponds to a protein fusion between the *Dpp* signal peptide and the GFP coding sequence (Entchev et al., 2000). We found that Hh-Np strongly colocalizes with sGFP in large vesicles (Figure 7A). Interestingly, this colocalization is restricted to a median level in the cell depth (Figure 7A″, arrows), while, more apically, less colocalization is present (Figures 7A and 7A′). This suggests that, initially, Hh-Np might follow the secretory pathway similarly to sGFP but might then use a different route to reach the apical surface of the cell.

In order to assess whether the Hh-Np LPSs might represent its concentration in caveolae-like structures, we compared LPS distribution with that of *Drosophila* Flotillin (Flo^{Dm}). Flo^{Dm} is an integral membrane protein that has been shown to contribute to the structural organization of caveolae when expressed in mammalian cells (Galbiati et al., 1998). However, we were unable to detect any costaining between Flo^{Dm} and Hh-Np in wild-type embryos (Figures 7B–7B″). Finally, we used the human transferrin receptor (hTfR) as a marker for endocytic vesicles in *Drosophila* (Bretscher, 1996; Teleman and Cohen, 2000). After binding to its ligand, hTfR is internalized and recycled through early endosomes. The UAS-hTfR transgene was expressed in all ectodermal cells, except En/Hh cells, with the *ptcGal4* driver. hTfR is greatly enriched at the apical surface of the expressing cells and in internal vesicles (Figure 7C). Interestingly, Hh-Np LPSs are present in hTfR-positive vesicles at the apical and subapical surface of the receiving cells that are adjacent to the source of Hh (Figure 7C and 7C′, arrows). Hence, these data suggest that Hh-Np LPSs are internalized by endocytic process.

Discussion

In this study we present evidence for the functional role of cholesterol modification in the control of Hh subcellular localization in the embryonic epithelium. We demonstrate that cholesterol modification is required for Hh assembly into LPSs and its apical targeting in a Disp-dependent manner. Furthermore, we show that LPS apical movement requires Ttv-dependent proteoglycans and that this movement is necessary for adjacent anterior cells to receive Hh input and express *wg*. In contrast,

basolateral Hh localization is sufficient for *rho* activation in adjacent posterior cells, independent of cholesterol modification of Hh.

Role of Hh Palmitoylation

In certain developmental processes, palmitoylation increases Hh activity to reach the threshold necessary for target gene expression (Kohtz et al., 2001; Lee et al., 2001; Taylor et al., 2001). Here we show that expressing C85S-Hh-Np lacking palmitic acid modification can rescue *hh* loss-of-function during embryogenesis, though less efficiently than a wild-type Hh molecule (Figures 2 and 3). Hence, as in vertebrates, palmitic acid modification potentiates Hh activity in *Drosophila* embryos. In contradiction with our data, Lee et al. (2001) observed that the C85S-Hh-Np construct is unable to rescue *hh* mutant embryos. This result is probably due to the use of the *enGal4* driver, which transiently depends upon the Hh and Wg regulatory loop (Heemskerk et al., 1991), instead of the Hh-independent driver used in our study. Using *enGal4*, we also observed a weak and variable rescue of *wg* expression and cuticle patterning in *hh* mutant embryos (data not shown). Interestingly, Hh-N is rendered inactive if not palmitoyled (Figure 3D, C85S-Hh-N; data not shown), suggesting that palmitoylation occurs independently of cholesterol modification.

Different Subcellular Localizations of Hh

We show that Hh is localized at the basolateral membrane of producing cells. Hh is also present in LPS, the formation of which is cholesterol dependent. Since we did not observe any difference in LPS formation with a nonpalmitoyled C85S-Hh-Np construct, the cholesterol modification on Hh appears to be the main requirement for Hh targeting to LPSs. Rietveld et al. (1999) identified two different fractions of membrane-bound Hh in *Drosophila*: a detergent-insoluble fraction corresponding to lipid raft microdomains and a detergent-soluble fraction. Therefore, a potential hypothesis would be that the Hh LPSs correspond to cholesterol-enriched raft microdomains. Nevertheless, we were unable to show any colocalization of Hh with Flo^{Dm}, the fly homolog of raft-associated caveolin. We were also unable to see any Hh-related cuticle defects in embryos injected with drugs known to deplete cholesterol and, thus, lipid raft microdomains (methyl-β-cyclodextrin and filipin; data not shown).

The assembly and the apical sorting of Hh-Np LPSs are dependent upon both cholesterol and Disp activity (Figures 4 and 5). However, Disp is not necessary for cholesterol binding to Hh (Burke et al., 1999). In *C. elegans*, the *disp* homolog (*CHE-14*; Michaux et al., 2000) is required for apical cuticle secretion. Therefore, one tempting possibility might be that the SSD on Disp specifically recognizes cholesterol-modified Hh for its assembly into LPSs and apical sorting. Since Hh-Np is still present on basolateral membranes in *disp* mutants (Figure 5), formation of LPSs could start from these locations before apical sorting. Alternatively, two independent routes could be responsible for basolateral and apical targeting (Figure 8).

Our results are in disagreement with previous work showing that Hh is evenly distributed between apical and basolateral surfaces in the developing *Drosophila* wing disc (Burke et al., 1999). We have found that Hh-Np is enriched at the apical surface in the posterior compartment of wild-type discs (data not shown). We have also detected apical LPSs in the anterior compartment (near the anteroposterior boundary, as previously shown in Tabata and Kornberg, 1994) of wild-type discs, which are completely lost in *disp* mutant discs (data not shown). These differences could be accounted for by the use of different Hh antibodies and by the use in Burke's study of an HA-tagged Hh that might not reflect all Hh biological activity.

Hh Movement through the Cellular Field

Cholesterol-dependent Hh-Np LPSs require Ttv to diffuse in the cellular field (Figure 6). How can Hh-Np be released from cells if it is inserted in the lipid bilayers? The mechanism of release might involve either a displacement of the cholesterol tether on Hh-Np or the formation of membrane vesicles. So far, no evidence for vesiculation has been reported, but large soluble multimers of Shh-Np have been identified in conditioned media of vertebrate cells (Zeng et al., 2001). Multimers of Hh-Np are also present in conditioned culture media from Hh-producing *Drosophila* Schneider cells (data not shown). Furthermore, the fact that all Shh or Hh soluble molecules identified so far are cholesterol-modified strongly suggests that Hh-Np cannot be released from its anchor by cleavage.

How do Hh-Np LPSs move within the cellular field? At least two alternative mechanisms could explain this movement. Planar transcytosis and, thus, transit from cell to cell in an endocytic and recycling-dependent manner might be involved. Alternatively, Hh-Np LPSs could pinch off from membrane raft domains, spread in the extracellular space, and become internalized away from the source at different cell positions (Figure 8). The role of the Ttv-dependent heparan sulfates could either be to stabilize such structures or to transport them from cell to cell.

Different Hh Target Gene Activation Is Dependent upon Apicobasal Sorting

Differential activation of *wg* and *ptc* in anterior cells and of *rho* and *ptc* in posterior cells is related to the membrane localization of Hh. We show that cholesterol-dependent LPS formation and apical targeting are necessary for proper anterior *wg* activation but dispensable for *rho* expression in posterior cells. Conversely, basolateral targeting of Hh in cells producing Hh-N-CD2 and Hh-N-GPI (Figure 4) is sufficient to activate the posterior *rho* expression, independent of the presence of cholesterol (Figure 2 and data not shown).

Interestingly, *wg* is expressed in adjacent cells located just anterior to the Hh-sending cells. Hence, long-range diffusion of Hh should not be required for *wg* activation. However, we show that, in absence of Ttv function, Hh-Np LPSs are blocked apically in producing cells, and *wg* is not activated (Figure 6). Ttv-dependent heparan sulfate proteoglycans are required for long-range Hh-Np movement in the wing disc (Bellaiche et al., 1998). Thus, our results suggest that, in the embryonic ectoderm, two different mechanisms of Hh pathway activation are present. *wg* activation requires all the events

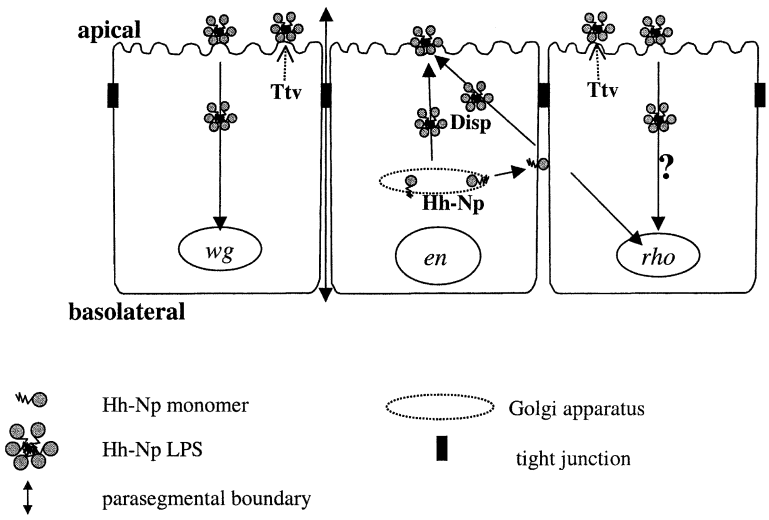

Figure 8. A Model for Hh-Np Trafficking

Maturation of the Hh precursor in *en* cells leads to its targeting to the Golgi apparatus, where it is cleaved and modified by palmitic acid and cholesterol to produce Hh-Np peptide (Jeong and McMahon, 2002). Hh-Np is sorted to the basolateral membrane, from where it can activate *rho* transcription in posterior cells. Disp organizes Hh-Np in LPSs (that might be related to vesicles or multimers). Disp might also be involved in LPS targeting to the apical surface. LPS assembly could occur at the basolateral or Golgi membranes. Hh-Np-containing LPSs are secreted and move through Ttv-dependent proteoglycan activity, thereby allowing Hh-Np to stimulate *wg* transcription in anterior cells. Although Ttv is not necessary for *rho* expression, it is possible that LPS activates the Hh pathway posterior to the Hh source (question mark).

previously associated with long-range Hh target gene activation and thus depends on Hh secretion and transport mechanisms. On the other hand, *rho* does not require secretion of Hh and can be activated in a cell-cell contact-dependent manner, like a short-range target (Figure 8). This difference could be due to differential accessibility of Hh to anterior versus posterior cells caused by the presence of the parasegmental boundary between *en* and *wg* cells (Ingham and Martinez Arias, 1992). Indeed, when Ttv is expressed exclusively in cells anterior to En cells, both *wg*- and *rho*-dependent cell differentiation are rescued. This indicates that a differential transport and/or presentation of Hh-Np could be responsible for the asymmetric cellular response to Hh.

How then is *rho* activated in cells posterior to Hh-producing cells? *rho* expression could depend on cell-cell contact activation with or without internalization of Hh. Although no detectable Hh in Hh-N-CD2 neighboring cells was observed, we cannot exclude that *rho* activation might depend on Hh internalization. It is worth mentioning that an Shh-CD4 transmembrane fusion protein has been shown to be internalized in adjacent cells through Ptc-1 activity in mammalian tissue culture cells (Incardona et al., 2000) and could induce formation of the most posterior digit of the chick limb (Yang et al., 1997). Moreover, expression of Hh-Np in *disp* mutant embryos that are defective in apical sorting induces *rho* expression in several rows of cells. In these embryos small dots of Hh-Np are seen outside the producing cells, confirming a possible internalization of Hh in posterior receiving cells through basolateral membrane interactions. This internalization could propagate at long range, since *rho* and *ptc* are activated in six to seven rows of cells when non-cholesterol-modified Hh-N is expressed in *disp* mutant embryos (Figure 5 and data not shown).

In summary, our data suggests that some Hh/Shh targets can be activated through Hh trafficking in LPSs followed by apical secretion, whereas other targets might be activated by basolaterally targeted Hh. Hence, we hypothesize that presentation of Hh from different cellular membrane compartments allows the receiving cells to differentially respond to the Hh input. This provides an interesting new paradigm regarding the mode of action of morphogens in all metazoans.

Experimental Procedures

Drosophila Stocks

hh^{AC}, hh^{15}, $disp^{377w+}$, and ttv^{00681} are null alleles (Lee et al., 1992; Mohler, 1988; Burke et al., 1999; Thé et al., 1999). Stocks are described in Burke et al. (1999) for *FRT82B* $disp^{377w+}$*/TM6B* and *UAS-hh-N-GPI*, Thé et al. (1999) for *FRTG13* ttv^{00681}*/CyOftzlacZ* and ttv^{00681} *enGal4/CyO*, Ingham and Fietz (1995) for *UAS-*hh^{FL}, Strigini and Cohen (1997) for *UAS-hh-N-CD2*, Entchev et al. (2000) for *UAS-sGFP*, and Teleman and Cohen (2000) for *UAS-hTfR*. *UAS-hh-N*, *UAS-C85S-hh-Np*, and *UAS-C85S-hh-N* transgenic flies were obtained by germline P element injection. Several independent transgenic lines were tested for each *hh* construct and gave similar results. Other stocks were obtained from the Bloomington stock center.

Genetic Experiments

Germline clones were obtained as described in Chou and Perrimon (1996) with the *hsp-70 flp101* flipase located on the X chromosome. The following strains carrying recombinant chromosome (in order to easily identify mutant embryos) were obtained by classical genetic techniques*: w; 69BGal4* hh^{AC}*/TM3 Sb Ser*, *w; UAS-lacZ;* hh^{15} *UAS-*hh^{FL}*/TM2*, *w;* hh^{AC} *UAS-hh-N-GPI/TM2*, *w;* hh^{AC} *UAS-hh-N-CD2/TM3 Sb Ser*, *w;* hh^{AC} *UAS-C85S-*hh^{FL}*/TM3 Sb Ser*, and *w;* hh^{AC} *UAS-C85S-hh-N/TM3 Sb Ser*.

Cuticle Preparation, In Situ Hybridization, and Protein Detection

Cuticle preparation, immunostaining, and RNA in situ hybridization were performed as in Gallet et al. (2000). *wg*, *ser*, and *rho* antisense RNA probes were made from pBluescript plasmid (gifts from S. Chauvet and Y. Graba for *wg* and from J.P. Vincent for *rho* and *ser*) with T3 polymerase. *ptc* antisense RNA probe was made from the *ptc*-pNB40 plasmid with T7 polymerase. Antibodies were used at the following dilutions: mouse 4D9 monoclonal anti-Engrailed (1/100; gift from M. Bourouis); mouse 4D4 monoclonal anti-Wg (1/20; Developmental Studies Hybridoma Bank, University of Iowa); mouse monoclonal JB10 anti-Nrt (1/200; gift from A. LeBivic); rabbit "Calvados" polyclonal anti-Hh (1/500), mouse monoclonal anti-Flotillin-1 (1/40), and anti-CD71 (hTfR; 1/100) from BD Biosciences; alkaline phosphatase-coupled anti-Dig (1/1000; Roche); secondary biotin conjugated (1/1000; Jackson Laboratory). Vector kits were used for peroxydase staining. FITC-conjugated goat anti-mouse (1/200), Cy3-conjugated goat anti-rabbit (1/400), and Rhodamine Red-X-conjugated Streptavidin (1/100) fluorescent secondary antibodies

(Jackson Laboratory) were used. Fluorescent images were obtained with a Leica DMR TCS_NT confocal microscope. In each experiment employing *disp*, *hh*, or *ttv* mutant embryos, we identified embryos of the correct genotype by the loss of some En/Hh-expressing cells.

Generation of Anti-Hh Sera from Rabbit

The Hh coding sequence from amino acid 85 to 257 was cloned into pRSET A vector in phase with a His_6 tag (Invitrogene). BL21 DE3 pLysS *E. coli* strain was used for recombinant protein production. Ni-NTA resin (Qiagen) was used for the His_6-tagged Hh purification by standard protocol under denaturing conditions. Two rabbits were immunized, and blood samples were analyzed after several boosts. Results shown in this study were obtained with serum from one rabbit, named "Calvados".

Mutagenesis

The C85S mutation on hh^{FL} was made by site-directed mutagenesis with the GeneEditor kit (Promega) and an oligonucleotide with the following sequence: 5′-GCCCGGCTCACAGCTCCGGACCTGGCCG AGGATTGG-3′. The wild-type TGC codon, which specifies cysteine, was replaced by a TCC codon, which specifies serine. *C85S-hh*^{FL} was then inserted into pUAST with EcoRI and KpnI. The *C85S-hh-N* construct was made by PCR amplification of the *C85S-hh*^{FL} with oligonucleotides with the sequence 5′-GGAATTCATGGATAACCAC AGCTCA-3′ and 5′-GGGTACCTCAGCCGTGCACGTGGGA-3′. In the second oligonucleotide, the TGC codon, which specifies cysteine, was replaced by a TGA codon, which specifies a stop. The amplified fragment was cloned in PGM-T Easy vector (Promega) and then cloned with EcoRI into pUAST. Both constructs were confirmed by sequencing.

Acknowledgments

We are grateful to K. Basler, J. Treisman, S. Cohen, M. Gonzalez-Gaitan, I. Thé, and N. Perrimon for fly stocks and to A. LeBivic and M. Bourouis for antibodies. We thank L. Staccini-Lavenant for technical help. We would like to thank P. Leopold, S. Noselli, and, especially, N. Tapon for helpful comments on the manuscript. We also thank all "fly" members of the ISDBCR for exciting discussions about this work. A.G. was supported by a fellowship from l'Association pour la Recherche sur le Cancer (ARC), and R.R. was supported by a doctoral fellowship from the French Research Ministry. This work was supported by grants from ARC, Fondation de France, and the ATIPE program of the Centre National de la Recherche Scientifique to P.P.T.

Received: July 31, 2002
Revised: November 25, 2002

References

Beachy, P.A., Cooper, M.K., Young, K.E., von Kessler, D.P., Park, W.J., Hall, T.M., Leahy, D.J., and Porter, J.A. (1997). Multiple roles of cholesterol in hedgehog protein biogenesis and signaling. Cold Spring Harb. Symp. Quant. Biol. *62*, 191–204.

Bellaiche, Y., Thé, I., and Perrimon, N. (1998). Tout-velu is a Drosophila homologue of the putative tumour suppressor EXT-1 and is needed for Hh diffusion. Nature *394*, 85–88.

Brand, A.H., and Perrimon, N. (1993). Targeted gene expression as a means of altering cell fates and generating dominant phenotypes. Development *118*, 401–415.

Bretscher, M.S. (1996). Expression and changing distribution of the human transferrin receptor in developing Drosophila oocytes and embryos. J. Cell Sci. *109*, 3113–3119.

Burke, R., Nellen, D., Bellotto, M., Hafen, E., Senti, K.A., Dickson, B.J., and Basler, K. (1999). Dispatched, a novel sterol-sensing domain protein dedicated to the release of cholesterol-modified hedgehog from signaling cells. Cell *99*, 803–815.

Chamoun, Z., Mann, R.K., Nellen, D., von Kessler, D.P., Bellotto, M., Beachy, P.A., and Basler, K. (2001). Skinny hedgehog, an acyltransferase required for palmitoylation and activity of the hedgehog signal. Science *2*, 2.

Chou, T.B., and Perrimon, N. (1996). The autosomal FLP-DFS technique for generating germline mosaics in Drosophila melanogaster. Genetics *144*, 1673–1679.

Entchev, E.V., Schwabedissen, A., and Gonzalez-Gaitan, M. (2000). Gradient formation of the TGF-beta homolog Dpp. Cell *103*, 981–991.

Forbes, A.J., Nakano, Y., Taylor, A.M., and Ingham, P.W. (1993). Genetic analysis of hedgehog signalling in the Drosophila embryo. Dev. Suppl., 115–124.

Galbiati, F., Volonte, D., Goltz, J.S., Steele, Z., Sen, J., Jurcsak, J., Stein, D., Stevens, L., and Lisanti, M.P. (1998). Identification, sequence and developmental expression of invertebrate flotillins from Drosophila melanogaster. Gene *210*, 229–237.

Gallet, A., Angelats, C., Kerridge, S., and Therond, P.P. (2000). Cubitus interruptus-independent transduction of the Hedgehog signal in Drosophila. Development *127*, 5509–5522.

Greco, V., Hannus, M., and Eaton, S. (2001). Argosomes: a potential vehicle for the spread of morphogens through epithelia. Cell *106*, 633–645.

Hatini, V., and DiNardo, S. (2001). Divide and conquer: pattern formation in Drosophila embryonic epidermis. Trends Genet. *17*, 574–579.

Heemskerk, J., DiNardo, S., Kostriken, R., and O'Farrell, P.H. (1991). Multiple modes of *engrailed* regulation in the progression towards cell fate determination. Nature *352*, 404–410.

Incardona, J.P., Lee, J.H., Robertson, C.P., Enga, K., Kapur, R.P., and Roelink, H. (2000). Receptor-mediated endocytosis of soluble and membrane-tethered Sonic hedgehog by Patched-1. Proc. Natl. Acad. Sci. USA *97*, 12044–12049.

Ingham, P.W., and Martinez Arias, A. (1992). Boundaries and fields in early embryos. Cell *24*, 221–235.

Ingham, P.W., and Fietz, M.J. (1995). Quantitative effects of hedgehog and decapentaplegic activity on the patterning of the Drosophila wing. Curr. Biol. *5*, 432–440.

Ingham, P.W., and McMahon, A.P. (2001). Hedgehog signaling in animal development: paradigms and principles. Genes Dev. *15*, 3059–3087.

Jeong, J., and McMahon, A.P. (2002). Cholesterol modification of Hedgehog family proteins. J. Clin. Invest. *110*, 591–596.

Kohtz, J.D., Lee, H.Y., Gaiano, N., Segal, J., Ng, E., Larson, T., Baker, D.P., Garber, E.A., Williams, K.P., and Fishell, G. (2001). N-terminal fatty-acylation of sonic hedgehog enhances the induction of rodent ventral forebrain neurons. Development *128*, 2351–2363.

Kuwabara, P.E., and Labouesse, M. (2002). The sterol-sensing domain: multiple families, a unique role? Trends Genet. *18*, 193–201.

Lee, J.D., Kraus, P., Gaiano, N., Nery, S., Kohtz, J., Fishell, G., Loomis, C.A., and Treisman, J.E. (2001). An acylatable residue of Hedgehog is differentially required in Drosophila and mouse limb development. Dev. Biol. *233*, 122–136.

Lee, J.J., von Kessler, D.P., Parks, S., and Beachy, P.A. (1992). Secretion and localized transcription suggest a role in positional signaling for products of the segmentation gene hedgehog. Cell *71*, 33–50.

Lewis, P.M., Dunn, M.P., McMahon, J.A., Logan, M., Martin, J.F., St-Jacques, B., and McMahon, A.P. (2001). Cholesterol modification of sonic hedgehog is required for long-range signaling activity and effective modulation of signaling by Ptc1. Cell *105*, 599–612.

Lind, T., Tufaro, F., McCormick, C., Lindahl, U., and Lidholt, K. (1998). The putative tumor suppressors EXT1 and EXT2 are glycosyltransferases required for the biosynthesis of heparan sulfate. J. Biol. Chem. *273*, 26265–26268.

Ma, Y., Erkner, A., Gong, R., Yao, S., Taipale, J., Basler, K., and Beachy, P.A. (2002). Hedgehog-mediated patterning of the mammalian embryo requires transporter-like function of dispatched. Cell *111*, 63–75.

McCormick, C., Leduc, Y., Martindale, D., Mattison, K., Esford, L.E., Dyer, A.P., and Tufaro, F. (1998). The putative tumour suppressor EXT1 alters the expression of cell-surface heparan sulfate. Nat. Genet. *19*, 158–161.

Michaux, G., Gansmuller, A., Hindelang, C., and Labouesse, M. (2000). CHE-14, a protein with a sterol-sensing domain, is required

for apical sorting in *C. elegans* ectodermal epithelial cells. Curr. Biol. *10*, 1098–1107.

Mohler, J. (1988). Requirements for hedgehog a segmental polarity gene in patterning larval and adult cuticle of Drosophila. Genetics *120*, 1061–1072.

Müller, H.A., and Wieschaus, E. (1996). armadillo, bazooka, and stardust are critical for early stages in formation of the zonula adherens and maintenance of the polarized blastoderm epithelium in Drosophila. J. Cell Biol. *134*, 149–163.

Pepinsky, R.B., Zeng, C., Wen, D., Rayhorn, P., Baker, D.P., Williams, K.P., Bixler, S.A., Ambrose, C.M., Garber, E.A., Miatkowski, K., et al. (1998). Identification of a palmitic acid-modified form of human Sonic hedgehog. J. Biol. Chem. *273*, 14037–14045.

Porter, J.A., Ekker, S.C., Park, W.J., von Kessler, D.P., Young, K.E., Chen, C.H., Ma, Y., Woods, A.S., Cotter, R.J., Koonin, E.V., and Beachy, P.A. (1996). Hedgehog patterning activity: role of a lipophilic modification mediated by the carboxy-terminal autoprocessing domain. Cell *86*, 21–34.

Rietveld, A., Neutz, S., Simons, K., and Eaton, S. (1999). Association of sterol- and glycosylphosphatidylinositol-linked proteins with Drosophila raft lipid microdomains. J. Biol. Chem. *274*, 12049–12054.

Strigini, M., and Cohen, S.M. (1997). A Hedgehog activity gradient contributes to AP axial patterning of the Drosophila wing. Development *124*, 4697–4705.

Tabata, T., and Kornberg, T.B. (1994). Hedgehog is a signaling protein with a key role in patterning *Drosophila* imaginal discs. Cell *76*, 89–102.

Taylor, A.M., Nakano, Y., Mohler, J., and Ingham, P.W. (1993). Contrasting distributions of patched and hedgehog proteins in the Drosophila embryo. Mech. Dev. *42*, 89–96.

Taylor, F.R., Wen, D., Garber, E.A., Carmillo, A.N., Baker, D.P., Arduini, R.M., Williams, K.P., Weinreb, P.H., Rayhorn, P., Hronowski, X., et al. (2001). Enhanced potency of human Sonic hedgehog by hydrophobic modification. Biochemistry *40*, 4359–4371.

Teleman, A.A., and Cohen, S.M. (2000). Dpp gradient formation in the *Drosophila* wing imaginal disc. Cell *103*, 971–980.

Thé, I., Bellaiche, Y., and Perrimon, N. (1999). Hedgehog movement is regulated through tout velu-dependent synthesis of a heparan sulfate proteoglycan. Mol. Cell *4*, 633–639.

Yang, Y., Drossopoulou, G., Chuang, P.T., Duprez, D., Marti, E., Bumcrot, D., Vargesson, N., Clarke, J., Niswander, L., McMahon, A., and Tickle, C. (1997). Relationship between dose, distance and time in Sonic Hedgehog-mediated regulation of anteroposterior polarity in the chick limb. Development *124*, 4393–4404.

Zeng, X., Goetz, J.A., Suber, L.M., Scott, W.J., Jr., Schreiner, C.M., and Robbins, D.J. (2001). A freely diffusible form of Sonic hedgehog mediates long-range signalling. Nature *411*, 716–720.